

# Electrically tunable Multiquantum-Well InGaAsP/InGaAsP microphotonic filter

M. V. Kotlyar, L. O'Faolain, A. Krysa and T. F. Krauss

**Abstract**— Planar waveguide-based Fabry-Perot microcavities of 20  $\mu\text{m}$  and 40  $\mu\text{m}$  length have been studied. The cavity resonance has been tuned via carrier-injection by a maximum of 1.9 nm at a wavelength of 1.3  $\mu\text{m}$  with only 6 mW of tuning power. The interplay between electrical and thermal tuning is highlighted.

**Index Terms**—Fabry-Perot cavity, InGaAsP, tunable filters, quantum well devices, microresonators

## I. INTRODUCTION

TUNABLE microcavities and devices are important for the realization of microphotonic circuits. Various compact active devices based on microcavities, such as switches, modulators and attenuators have now been demonstrated [1, 2] and have shown operation at high speed and with low power consumption.

InP-based materials are particularly attractive for these applications because they exhibit several electro-optic effects, provide gain at the telecommunications wavelengths of 1.3 and 1.55  $\mu\text{m}$  and offer low thermal resistance.

Fabry-Perot (F-P) type resonators are frequently used as filters. For example, a tunable F-P resonator was recently realized in silicon on insulator (SOI) and experimentally tuned by carrier-injection [3]. Tuning of 0.8 nm was achieved for 20 mW of consumed power. The tuning mechanism, however, was thermo-optical rather than electronic, due to the relatively high thermal resistance of the examined device of around 1 K/mW. This interplay between thermal and electronic tuning in microphotonic deserves attention, because a) thermal tuning is typically much slower than electronic tuning, and b) the refractive index change for thermal and electronic tuning is of opposite sign in the commonly used semiconductors, so the two effects tend to compensate one another.

Here, we report on the fabrication and characterization of 20 and 40- $\mu\text{m}$ -long tunable F-P type filters in multiquantum well (MQW) InGaAsP/InGaAsP material. Due to the relatively low surface recombination velocity of InP-based material and good heat sinking, successful tuning of the cavity resonance was achieved using carrier injection. For higher currents, however, lasing takes place which clamps the carrier

density and prevents further blue-shifts. Thermal effects then take over that reverse the wavelength shift.

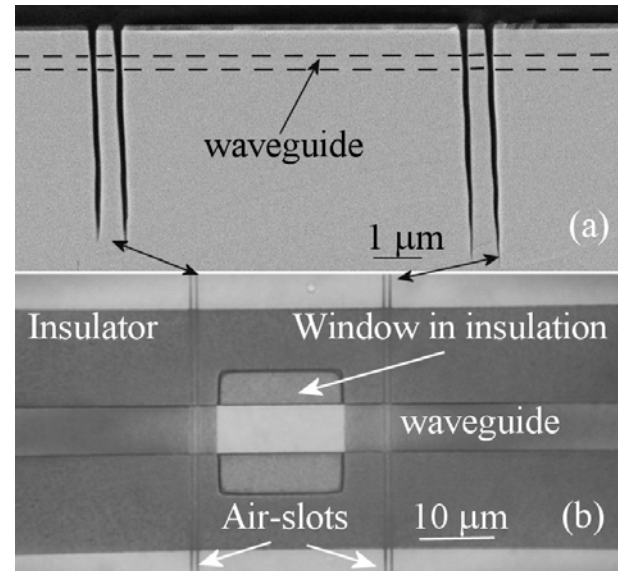


Fig. 1.(a) A scanning electron microscope image of the cross-section of a filter with a 10- $\mu\text{m}$  cavity. The slots were etched to the depth of 4  $\mu\text{m}$  using CAIBE, (b) a top view of a filter with a 20- $\mu\text{m}$  cavity prior to contact evaporation. The 5  $\mu\text{m}$  ridge waveguide, SU-8 insulator and air-slots for mirrors are clearly indicated.

Our device consists of a cavity (20  $\mu\text{m}$  or 40  $\mu\text{m}$  length) defined by third-order Bragg mirrors (Fig. 1). The air-slots forming the Bragg mirrors were kept small (100 nm) in order to minimize diffraction losses. The structure was written using electron-beam lithography with polymethylmethacrylate (PMMA) as a resist and transferred into a SiO<sub>2</sub> hard-mask using reactive ion etching (RIE). The slots were etched up to 4  $\mu\text{m}$  deep using chemically assisted ion beam etching (CAIBE) (Fig. 1 (a)) [4].

Ridge waveguides (5  $\mu\text{m}$  width) were created using optical lithography (Fig. 1 (b)). Shallow (250 nm) etching was used to ensure single mode operation of the waveguide.

The waveguide core consists of 5 quaternary/quaternary 6.5-nm wide InGaAsP/InGaAsP QWs. The band-gap wavelengths of QWs and barriers are 1.3 and 1.1  $\mu\text{m}$ , respectively. A Ni/Au top contact and an Au/Ge/Ni bottom contact were used. The contacts were large rectangles (70 by 100  $\mu\text{m}$ ) with an SU-8 polymer electrical insulation.

Manuscript received September 21, 2004.

M. V. Kotlyar, L. O'Faolain and T. F. Krauss are with School of Physics and Astronomy, University of St Andrews, North Haugh, St. Andrews, Fife KY 16 8 SS, UK (e-mail: mvk@st-andrews.ac.uk).

A. Krysa is with Dept. of Electronic Engineering, University of Sheffield, Mappin St, Sheffield S1 3JD, UK.

II. EXPERIMENTAL RESULTS AND ANALYSIS

A tunable laser operating between 1250-1365 nm was used to examine the devices. An experimental transmission spectrum of a device with 40 μm cavity with a full width half maximum (FWHM) of less than 2 nm is presented in Fig. 2. The free spectral range (FSR) is about 6 nm as expected. In order to have a larger FSR, smaller cavities can be used. 20-μm long cavities, for example exhibit an FSR of 12 nm. The height of the experimental transmission peaks is strongly influenced by the absorption spectrum of the material which has a peak of absorption near 1250 nm.

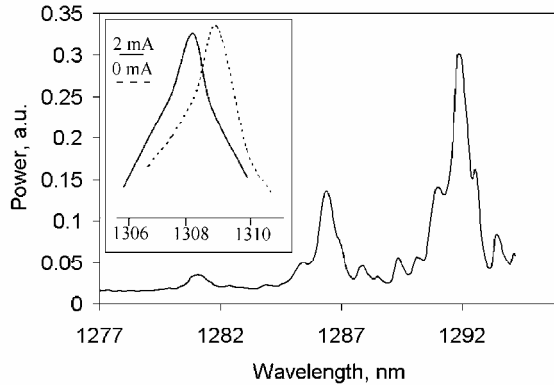


Fig. 2. A transmission spectrum of a passive filter with a 40-μm cavity, exhibiting a FWHM around 2 nm and a FSR of 6 nm. Proximity to the absorption peak of the material near 1250 nm affects the height of the transmission peaks. The inset shows a blue-shift of 0.7 nm for an injected current of 2 mA.

Applying a forward bias to the cavity, (the access waveguides were left un-pumped), creates carriers which are mostly collected inside the 5 QWs. Injected carriers cause changes in the absorption spectrum via bandfilling, band-gap shrinkage and free-carrier absorption [5]. Changes in the refractive index of the QWs result from these absorption spectrum changes, and are governed by the Kramers-Kronig relationship. For carrier densities of around  $3 \cdot 10^{18}/\text{cm}^3$  and close to the bandgap, the band-filling effect is predominant and provides the largest contribution to the refractive index changes.

Due to the relatively high Q-factor (~700) of the filter, the resonances of the optical mode in the resonator are very sensitive to even small changes in the refractive index of the medium, so the resonator acts as an “amplifier” of the carrier-induced effect.

The inset of Fig. 2 shows the measured carrier-induced blue shift of a single filter peak for TE-polarization. A shift of about 0.7 nm at 1309 nm was observed in a device with a 40-μm long cavity for an injected current of 2 mA, yet we failed to observe greater shifts of the transmission peak towards shorter wavelengths at higher currents. In fact, a reduced shift of 0.6 nm was observed for an injection current of 10 mA. This shift in the opposite direction can be explained by heating effects in the microcavity, as the thermally induced refractive

index change has the opposite sign to that of the carrier - induced shift (Fig. 3).

In Fig. 3 the refractive index decreases up to a tuning current of about 2 mA and then increases again for higher currents. We believe that this change of direction occurs because of the onset of lasing at about 2 mA, which was verified independently. At lasing threshold, the carrier density

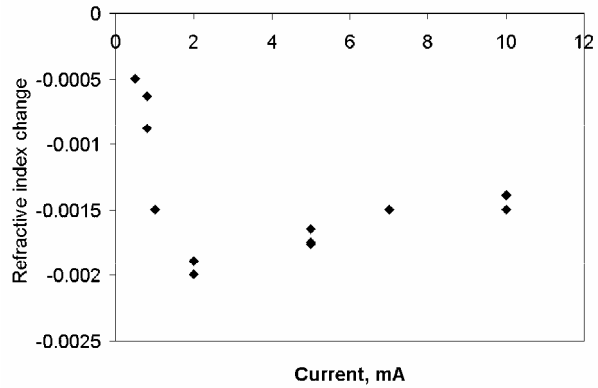


Fig. 3. Carrier-injection modal refractive index changes induced in a 40-μm cavity filter. Refractive index changes are given for the waveguide region. A pronounced thermally induced shift in the opposite direction appears after 2 mA.

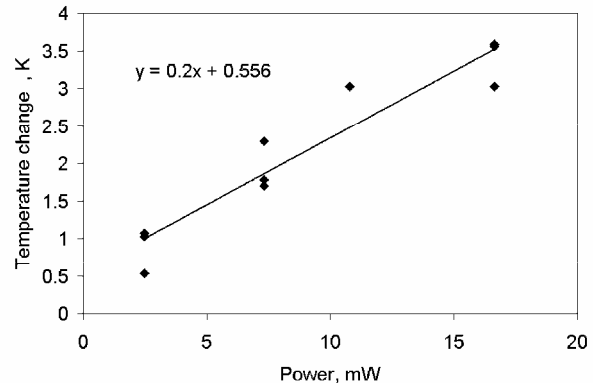


Fig. 4. Experimentally observed dependence of the cavity temperature change vs. dissipated power for a 40-μm cavity filter.

is clamped, so no further carrier-induced refractive index change can be expected. In our case, the blue shift of the transmission peak will therefore not exceed 0.7 nm, which corresponds to an  $\Delta n$  of -0.025 in the quantum wells or  $\Delta n$  of 0.002 taking the overlap factor of 8 % for TE-polarization into account (the overlap is only 5 % for TM-polarization, making modal refractive index changes even smaller for this polarization). Increasing the current further then causes thermo-optical effects that are opposite in sign, thereby reducing the observed shift. The rise in cavity temperature ( $\Delta T$ ) is connected with power dissipated ( $P_d$ ) in the cavity of a filter by:  $\Delta T = R_{th} \cdot P_d$ , where  $R_{th}$  is a thermal resistance of the device. At the same time  $\Delta n / \Delta T = K_{TO}$ , where  $K_{TO}$  is the thermo-optic coefficient. Thus, knowing  $K_{TO}$  for InGaAsP

(typically around  $2 \times 10^{-4} \text{ K}^{-1}$ ),  $\Delta T$  can be derived as a function of the dissipated power from the experimental data of  $\Delta n$  versus  $I$  (presented in Fig. 3). From the slope of the curve in Fig. 4 a thermal resistance of 0.2 K/mW can be calculated.

This resistance is less than half of the theoretical value of 0.5 K/mW extracted from a two-dimensional approximation of heat dissipation in the following form [6]:

$$R_{\text{thermal}} = \frac{Ln\left(\frac{4h}{w}\right)}{\pi * K * L} \quad (1)$$

Where  $h$  is the thickness of a wafer,  $w$  is a lateral dimension of carrier spreading,  $K$  is a thermal conductivity of InP and  $L$  is a cavity length. This approximation is valid when the total thickness of the wafer is well in excess of the size of the heat source.

We believe that the values of the thermal resistance (within experimental error) are smaller than theoretically predicted due to heat dissipation by the top contact pad which was deliberately oversized, thereby acting as a “cooling fin” [7].

The rate of change of the transmission peak shift is  $(\Delta\lambda/T) = 0.36 \text{ nm/mA}$ . For comparison, this value exceeds the value of  $\sim 0.09 \text{ nm/mA}$  for InGaAsP/InP F-P cavity reported by H. K. Tsang *et al.* [8] and is of the same order as that reported by K. Djordjev *et al.* [1].

Filters with shorter cavity lengths (20  $\mu\text{m}$ ) were also investigated. One of the advantages of this shorter cavity is the larger FSR (of 12 nm). The smaller cavity length also has a higher threshold current density allowing the injection of more current into the device giving an increased maximum carrier density. Thus, a blue-shift of 1.5 nm was experimentally observed for an injected current of 2.7 mA. However, at the same time the heating effect is more severe for smaller cavities due to an increased thermal resistance. The experimentally extracted thermal resistance for the 20  $\mu\text{m}$  cavity is about 0.4 K/mW (the theoretical value is 1 K/mW). This is two times larger than that of the 40- $\mu\text{m}$  cavity, as expected from (1).

Pulsed currents (10  $\mu\text{s}$  pulse width for 1000  $\mu\text{s}$  period) were used in order to reduce the heating problem and a blue-shift of 1.9 nm was obtained for an injection current of 2.69 mA. The difference between this value and the 1.5 nm blue shift obtained by the DC measurement, above, agrees well with the red shift (0.3 nm) caused by heating (calculated using the experimental thermal resistance of 0.4 K/mW measured above).

Several effects impact on the effectiveness of the carrier-induced index changes. The lateral spread of the current, the low overlap between the optical mode and the QWs ( $I \sim 8\%$ ) and the surface recombination of the carriers at the etched sidewalls minimize the overall refractive index changes we were able to observe.

Finally, larger shifts may be achieved by shifting the reflectivity peak of the mirrors, in order to suppress laser action at the gain peak, hence increasing the tuning range.

### III. CONCLUSION

In conclusion, F-P type filters were realized in an InGaAsP/InGaAsP MQW structure with deeply etched mirrors. A FWHM of less than 2 nm and a FSR of 12 nm was experimentally observed for a filter with a 20- $\mu\text{m}$  cavity. Using carrier injection, a shift of 1.5 nm (direct currents) and 1.9 nm (pulsed) were achieved for the filter consuming only 6 mW of power. A design with large contact pads (compared with the size of the cavities) allowed us to reach relatively small thermal resistances of 0.2 and 0.4 K/mW for filters with 20- and 40- $\mu\text{m}$  cavities, respectively. A material structure incorporating a larger number of QWs could be used to produce larger wavelength shifts, because of the increased overlap with the optical mode and the higher current required for lasing and thus thermal tuning to occur. Overall, we have highlighted the limitations and opportunities for III-V semiconductor based tunable microphotonic circuit elements by demonstrating a low power tunable filter in the 1.3  $\mu\text{m}$  wavelength regime.

### REFERENCES

- [1] K. Djordjev, S.-J. Choi, S.-J. Choi, and P.D. Dapkus, “Microdisk tunable resonant filters and switches”, *IEEE Photon. Technol. Lett.*, vol. 14, pp. 828-830, June 2002
- [2] T. A. Ibrahim, W. Cao, Y. Kim, J. Li, J. Goldhar, P.-T. Ho and C. H. Lee, “Lightwave switching in semiconductor microring devices by free carrier injection”, *J. Lightwave Technol.*, vol. 21, pp. 2997-3003, December 2003
- [3] C. A. Barrios, V. R. Almeida, R. R. Panepucci, B. S. Schmidt, and M. Lipson, “Compact Silicon Tunable Fabry-Perot Resonator with low power consumption”, *IEEE Photon. Technol. Lett.*, vol. 16, pp. 506-508, February 2004
- [4] M. V. Kotlyar, L. O’Faolain, R. Wilson, and T. F. Krauss “High-aspect-ratio chemically assisted ion-beam etching for photonic crystals using a high beam voltage-current ratio”, *JVST(B)*, vol. 22, pp. 1788-1791, July 2004
- [5] B. R. Bennett, R. A. Soref, and J. A. Del Alamo “Carrier-induced change in refractive index of InP, GaAs, and InGaAsP” *IEEE J. Quant. Electr.*, vol. 26, pp. 113-122, January 1990
- [6] L. A. Coldren and S. W. Corzine, *Diode Lasers and Photonic Integrated Circuits*, ser. Wiley Series in microwave and optical engineering. New York: J. Wiley, 1995.
- [7] K. P. Pipe and R. J. Ram “Comprehensive heat exchange model for a semiconductor laser diode” *IEEE Phot. Technol. Lett.*, **15** 504 (2003)
- [8] H. K. Tsang, M. W. Mak, L. Y. Chan, J. B. D. Soole, C. Youtsey, and I. Adesida “Etched cavity InGaAsP/InP Waveguide Fabry-Perot filter tunable by current injection” *J. Lightwave Technol.*, vol. 17, pp. 1890-1895, October 1999.